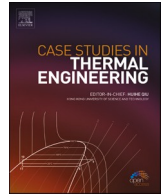




ELSEVIER

Contents lists available at ScienceDirect

Case Studies in Thermal Engineering

journal homepage: www.elsevier.com/locate/csited

Thermal radiation effect on Viscoelastic Walters'-B nanofluid flow through a circular cylinder in convective and constant heat flux

Rahimah Mahat^{a,*}, Muhammad Saqib^b, Ilyas Khan^c, Sharidan Shafie^b,
Nur Azlina Mat Noor^b

^a Universiti Kuala Lumpur Malaysian Institute of Industrial Technology, Persiaran Sinaran Ilmu, Bandar Seri Alam, 81750, Masai, Johor, Malaysia

^b Department of Mathematical Sciences, Faculty of Science, Universiti Teknologi Malaysia, 81310, UTM Johor Bahru, Johor, Malaysia

^c Faculty of Mathematics and Statistics, Ton Duc Thang University, Ho Chi Minh City, Viet Nam

ARTICLE INFO

Keywords:

Viscoelastic Walters'- B nanofluid
Sodium carboxymethyl cellulose
Thermal radiation
Convective boundary condition

ABSTRACT

The investigation on flow of nanofluid are well known amongst researchers due to its utilization in the industrial and engineering sector. It is useful for cooling purposes in the electronic devices, which has shown good results in energy saving. Thus, this study focusses on the analysis of radiation effects on mixed convection of Walters'-B nanofluid flow through a circular cylinder in the constant heat flux (CHF) and convective boundary conditions (CBC) horizontally. The sodium carboxymethyl cellulose (CMC-water) nanofluid is considered as conventional fluid containing copper nanoparticles. The numerical method of Keller-box is conducted to simplify the partial differential equations. Graphical profiles are plotted and discussed to examine the impacts of various physical terms on velocity, skin friction, temperature and thermal transfer. The results discover the fluid velocity and temperature boost for increasing radiation and Biot number caused by the raise of energy supply in the fluid flow. The velocity profile decreases when nanoparticles volume fraction increases as the increment of fluid concentration slowing down the fluid flow. The convective heat transfers and skin friction increases as mixed convection parameter rises by varying the thermal boundary region. Furthermore, the temperature and velocity in CHF condition are comparatively higher than CBC condition.

Nomenclature

a	Radius
C_p	Specific heat of the fluid ($\text{Jkg}^{-1}\text{k}^{-1}$)
C_f	Skin friction coefficient
h_f	Convective heat transfer
K	Viscoelastic parameter
k	Thermal conductivity of fluid
k^*	Coefficient of mean absorption
k_f	Heat conduction of base fluid
k_0	Viscoelasticity (kg/ms^2)

* Corresponding author.

E-mail address: rahimahm@unikl.edu.my (R. Mahat).

<https://doi.org/10.1016/j.csited.2022.102394>

Received 10 April 2022; Received in revised form 24 August 2022; Accepted 27 August 2022

Available online 8 September 2022

2214-157X/© 2022 The Authors. Published by Elsevier Ltd. This is an open access article under the CC BY-NC-ND license (<http://creativecommons.org/licenses/by-nc-nd/4.0/>).

k_{nf}	Heat conduction of nanofluid
N_R	Thermal radiation
Pr	Prandtl number
q_w	Wall heat flux
q_r	Radiative heat flux
Re	Reynolds number
T_f	Wall temperature (K)
T_∞	Ambient temperature (K)
T	Fluid temperature (K)
U_∞	Velocity at free stream (m/s)
\bar{u}	Velocity (x direction) (m/s)
u	Dimensionless velocity (x direction) (m/s)
\bar{v}	Velocity (y direction)
v	Dimensionless velocity (y direction)
\bar{x}	Coordinate of cylinder surface from lower stagnation point
\bar{y}	Coordinate normal to the cylinder surface
(x,y)	Cartesian coordinate
<i>Greek symbol</i>	
β_{nf}	Volumetric coefficient of thermal expansion of nanofluid
γ_1	Biot number
λ	Mixed convection parameter
ψ	Stream function
μ_{nf}	Dynamic viscosity of nanofluid
ρ_s	Solid fraction density of solid fraction
ρ	Fluid density (kg/m ⁻³)
ρ_f	Base fluid density
ρ_{nf}	Nanofluid density
φ	Nanoparticles volume fraction
σ^*	Stefan-Boltzman constant
τ_w	Wall skin friction
θ	Dimensionless temperature parameter
θ_w	Heat transfer coefficient

1. Introduction

The demand on high-energy devices have been grown expeditiously over a decade ago for a developing country. The thermal industrial devices which required high heat transfer capability are manufacturing, refrigerators, automotive, air-conditioning, aircraft and others high-energy devices. However, the traditional heat transfer approach cannot easily meet the high demands of these industrial devices [1]. Therefore, extensive studies have been carried out by research community to discover the best techniques to overcome these problems. After several attempts, many factors were identified which limit the traditional heat transfer approaches. One of the major factors limitations is low thermal conductivity in conventional fluids [2]. Common examples of conventional heat transfer fluid are ethylene glycol, oil and water. Therefore, the researchers suggested to improves the fluids thermal conductivity by dispersing nanoparticles into fluids to form suspension [3]. The suspension of nanometer-sized particles known as ‘nanofluid’ was proposed by Choi and Eastman [4]. The nanoparticles are made up of metal, oxide, carbide or carbon nanotube, which can flow smoothly through the micro channels [5]. Eventually, the utilization of nanofluid in high performance devices has received attention from many scientists due to its significance [6-7]. In this study, the non-Newtonian base fluid known as carboxymethyl cellulose-water (CMC-Water) is chosen. It exhibits higher ability to boost the convective heat transfer, thermal conductivity, diffusivity and viscosity compared to other base fluids [8-9].

The behavior of fluid is influenced by important mechanism known as convective heat transfer. The transfer of thermal energy amongst surface and fluid flow at different temperature is represented as convection. It is categorized in three different modes, free, force and mixed convection [10-11]. The fluid motion generated by free and forced convection is referred as mixed convection flow. It has been implemented in various industrial usages involving cooling of electronic devices by fan, a heat exchanger at the low velocity environment and solar collectors [12]. The research of convective heat transfer in fluid flow depends on boundary condition. Generally, two types of thermal boundary conditions are applied, convective boundary conditions (CBC) and constant heat flux (CHF). It is discovered that CBC arises when heat transfer at surface is proportional to temperature of local surface [13-14]. The studies on CBC and CHF have been discovered with various types of fluids, geometries, and impacts. Ramesh et al. [15] analyzed the flow on boundary layer across a stationary or moving inclined surfaces with CBC via shooting approach. The influences of CBC on mixed convection of

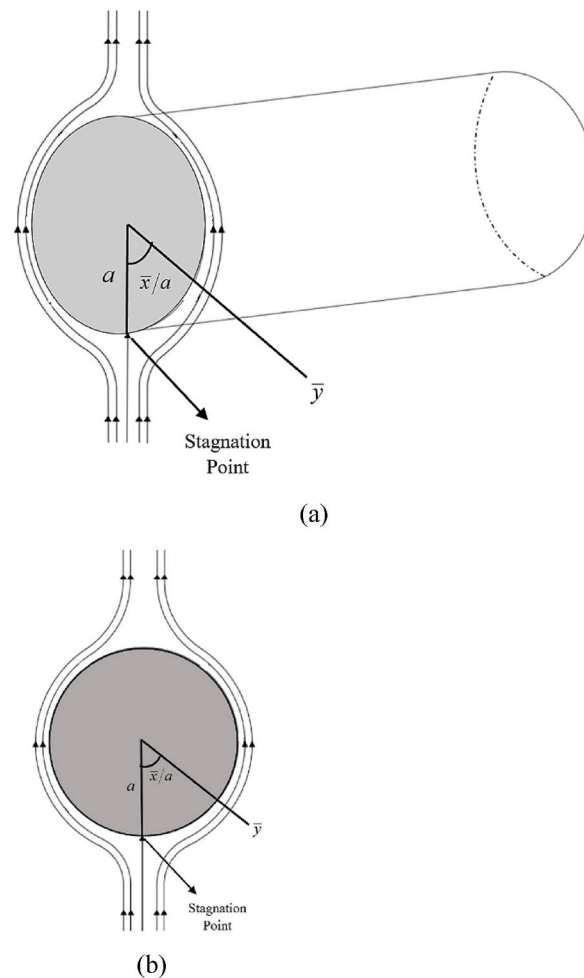


Fig. 1. The geometrical model of fluid across a circular cylinder in (a) three and (b) two dimension.

Casson fluid flow past a stretched surface with hall impact was examined by Ashraf et al. [16]. For the geometrical model of horizontal circular cylinder with CHF condition, Ahmad et al. [17] discovered convective flow and thermal transfer of viscoelastic fluid in the influences of radiation. Meanwhile, Zokri et al. [18] explored the convective flow of Jeffrey fluid with joule dissipation effect numerically.

The study of non-Newtonian fluids is prominent research amongst scientists due to its multiple usages in engineering, for example, fiber technology, geothermal energy extraction, coating of wires, biological fluids and oil reservoirs [19-20]. Viscoelastic Walters'-B fluid is a non-Newtonian fluid which describes both elastic and viscous properties. The pioneer work on Walters'-B was suggested by Rivlin [21] which explored the relation of stress deformation on isotropic materials. Later, Min et al. [22] extended Rivlin [21] works by studying limitations of Walters'-B fluid related to small deformation imposed on a large stretch. Co and Bird [23] pointed out that Walters'-B fluid does not move further and rapid from its initial configuration. Several researchers have conducted the studies on boundary layer flow of Walters'-B fluid using different geometrical models [24-33]. For circular cylinder geometry, the pioneer investigation on the flow of elastic-viscous Waters'-B fluid was reported by Harnoy [34]. Later, Nazar et al. [35] discovered the impacts of CHF on mixed convection viscous flow in a circular cylinder. Anwar et al. [36] extended Nazar et al. [35] works for both heated and cooled cases. Kasim et al. [37] continued Anwar's work [36] with presence of the constant heat flux condition. Later, Kasim et al. [38] extended their previous work by examining the impacts of heat source on the flow across circular cylinder.

The fluid flow with thermal radiation has gained the attentions of engineers because of its importance in engineering applications, including control heat transfer in the polymer process and nuclear reactor. The impacts of radiation in Casson fluid across a porous stretching sheet using Rosseland approximation was analyzed by Pramanik [39]. It is shown that convective heat transfer and temperature boosts for increasing radiation. Farooq et al. [40] investigated MHD viscoelastic nanofluid flow at a stagnation point with effect of radiation via homotopy analytical method (HAM). Kumar et al. [41] examined the influences of radiation on double-diffusive flows of viscoelastic nanofluid through a stretched surface by implementing Runge-Kutta Fehlberg and shooting techniques. Khan et al. [42] explored the chemical reaction and radiation impacts on Sisko fluid across a stretched permeable plate using HAM. Ibrahim et al. [43] discovered the influence of chemical reaction and radiation on non-Newtonian fluids with heat source, Soret and Dufour and slip

Table 1
Thermophysical properties of nanoparticle and base fluid.

Physical Properties	C_p (J kg ⁻¹ K ⁻¹)	ρ (kg m ⁻³)	k (Wm ⁻¹ K ⁻¹)	$\beta \times 10^5$ (K ⁻¹)
Nanoparticle (Cu)	385	8933	401	1.67
Base fluid (CMC-water)	4179	997.1	0.613	21

effects. The Casson and Williamson fluid flow is induced by a stretched plate with non-uniform thickness. Furthermore, Hussain et al. [44] analyzed the viscosity and thermal radiation on unsteady viscoelastic fluid over an infinite surface.

A literature survey discussed above reveals that limited study has been accounted on the flow of Walters'-B fluid through circular cylinder. Moreover, no work is conducted to examine the impacts of thermal radiation on viscoelastic Walters'-B nanofluid. Motivated by limitation of the studies, the present study explores the mixed convection flow and thermal transfer of Walters'-B nanofluid across a circular cylinder with thermal radiation impact. The convective and constant heat flux are considered as boundary conditions. The graphical and numerical solutions are obtained via MATLAB software. The influences of related dimensionless terms on fluid velocity, skin friction, temperature and thermal transfer rate are explored.

The present work is applicable to be implemented as the model for ultra-high cooling system. Nanofluid is very suitable as a coolant because of its properties, which are higher in thermal diffusivity and thermal conductivity compared to classic fluid. Cooling system in engine devices in one of the applications where nanofluid is used and plays an important role as a heat waste absorber in order to bring the engine temperature back to normal [45].

2. Mathematical formulation

Consider the flow of viscoelastic Walters'-B nanofluid through a circular cylinder. The definition of gravitational acceleration is $g_x = g \sin(\bar{x}/a)$. The velocity outer the region of boundary surface is $\bar{u}_e(\bar{x}) = U_\infty \sin(\bar{x}/a)$ with constant velocity $(1/2)U_\infty$ at free stream, which flow upward over the cylinder [11]. A three-dimensional model of viscoelastic Walter's-B nanofluid flow over a circular cylinder is displayed in Fig. 1(a). The cross-section view of Fig. 1(a) in two-dimension is presented in Fig. 1(b).

The governing equations of Walters'-B nanofluid are written as [49].

$$\frac{\partial \bar{u}}{\partial \bar{x}} + \frac{\partial \bar{v}}{\partial \bar{y}} = 0, \tag{1}$$

$$\bar{u} \frac{\partial \bar{u}}{\partial \bar{x}} + \bar{v} \frac{\partial \bar{u}}{\partial \bar{y}} = \bar{u}_e \frac{\partial \bar{u}_e}{\partial \bar{x}} + \frac{\mu_{nf}}{\rho_{nf}} \frac{\partial^2 \bar{u}}{\partial \bar{y}^2} - \frac{k_o}{\rho_{nf}} \left[\frac{\partial}{\partial \bar{x}} \left(\frac{\partial^2 \bar{u}}{\partial \bar{y}^2} \right) + \frac{\partial^3 \bar{u}}{\partial \bar{y}^3} - \frac{\partial \bar{u}}{\partial \bar{y}} \frac{\partial^2 \bar{u}}{\partial \bar{x} \partial \bar{y}} \right] + g \beta_{nf} (T - T_\infty) \sin \left(\frac{\bar{x}}{a} \right), \tag{2}$$

$$\bar{u} \frac{\partial T}{\partial \bar{x}} + \bar{v} \frac{\partial T}{\partial \bar{y}} = \frac{k}{\rho C_p} \frac{\partial^2 T}{\partial \bar{y}^2} + \frac{1}{\rho C_p} \frac{\partial q_r}{\partial \bar{y}} \tag{3}$$

with boundary conditions (BCs)

$$\left. \begin{aligned} \bar{u} = 0, \bar{v} = 0, -k_{nf} \frac{\partial T}{\partial \bar{y}} = h_f (T_f - T); \text{ at } \bar{y} = 0, \bar{x} \geq 0, \\ \bar{u} = \bar{u}_e(\bar{x}), \frac{\partial \bar{u}}{\partial \bar{y}} = 0, T = T_\infty; \text{ at } \bar{y} \rightarrow \infty, \bar{x} \geq 0, \end{aligned} \right\} \tag{4}$$

and

$$\left. \begin{aligned} \bar{u} = 0, \bar{v} = 0, T = -\frac{q_w}{k_{nf}}; \text{ at } \bar{y} = 0, \bar{x} \geq 0, \\ \bar{u} = \bar{u}_e(\bar{x}), \frac{\partial \bar{u}}{\partial \bar{y}} = 0, T = T_\infty; \text{ at } \bar{y} \rightarrow \infty, \bar{x} \geq 0, \end{aligned} \right\} \tag{5}$$

Note that the symbol '-' on the parameter refer to the dimensional parameter. Table 1 portrays the thermophysical properties of nanoparticle and base fluid [50].

The radiative heat transfer, q_r based on Rosseland approximation are expressed by [51].

$$\mathbf{q}_r = -\frac{4\sigma^*}{3k^*} \left[\frac{\partial T^4}{\partial \bar{x}}, \frac{\partial T^4}{\partial \bar{y}} \right], \tag{6}$$

The small difference of temperature in the fluid is indicated as T^4 . The variable T^4 is expanded as linear function via Taylor's series for T_∞ and written as

$$T^4 = T_\infty^4 + 4T_\infty^3 (T - T_\infty) + 6T_\infty^2 + \dots \tag{7}$$

Hence, the higher order terms are ignored yields

$$T^4 \cong 4T_\infty^3 T - 3T_\infty^4 \tag{8}$$

Then, substitute equations (6) and (8) into energy equation (3) obtain

$$\bar{u} \frac{\partial T}{\partial \bar{x}} + \bar{v} \frac{\partial T}{\partial \bar{y}} = \frac{k}{\rho C_p} \left(1 + \frac{16\sigma^* T_\infty^3}{3k^* k} \right) \frac{\partial^2 T}{\partial \bar{y}^2} \tag{9}$$

The similarity transformation is introduced to reduce the complexity of the governing coupled equations (1) to (3). Referring from Kanafiah et al. [52], Zokri et al. [53] and Selvakumar and Dhinakaran [54], the similarity variables are implemented to convert the partial differential equation into the ordinary differential equation. The similarity variables are

$$x = \bar{x}/a, y = \text{Re}^{1/2}(\bar{y}/a), u = \bar{u}/U_\infty, v = \text{Re}^{1/2}(\bar{v}/U_\infty), u_e(x) = \bar{u}_e(\bar{x})/U_\infty, \theta = (T - T_\infty)/(T_f - T_\infty), \theta = (T - T_\infty)\text{Re}^{1/2}/(aq_w/k_{nf}), \tag{10}$$

Substituting dimensionless variables (10) into equations (1), (2) and (9) gives the subsequent forms

$$\frac{\partial u}{\partial x} + \frac{\partial v}{\partial y} = 0 \tag{11}$$

$$\begin{aligned} \left[(1-\varphi) + \varphi \frac{\rho_s}{\rho_f} \right] \left[u \frac{\partial u}{\partial x} + v \frac{\partial u}{\partial y} \right] &= \left[(1-\varphi) + \varphi \frac{\rho_s}{\rho_f} \right] \sin x \cos x + \frac{1}{(1+\varphi)^{2.5}} \frac{\partial^2 u}{\partial y^2} \\ -K \left[\frac{\partial}{\partial x} \left(u \frac{\partial^2 u}{\partial y^2} \right) + v \frac{\partial^3 u}{\partial y^3} - \frac{\partial u}{\partial y} \frac{\partial^2 u}{\partial x \partial y} \right] &+ \left[(1-\varphi) + \varphi \frac{(\rho\beta)_s}{(\rho\beta)_f} \right] \lambda \theta \sin(x), \end{aligned} \tag{12}$$

$$\left[(1-\varphi) + \varphi \frac{(\rho C_p)_s}{(\rho C_p)_f} \right] \left[u \frac{\partial \theta}{\partial x} + v \frac{\partial \theta}{\partial y} \right] = \frac{(k_s + 2k_f) - 2\varphi(k_f - k_s)}{(k_s + 2k_f) + \varphi(k_f - k_s)} \frac{1}{\text{Pr}} \left(1 + \frac{4N_R}{3} \right) \frac{\partial^2 \theta}{\partial y^2} \tag{13}$$

with dimensionless BCs

$$\left. \begin{aligned} u = 0, v = 0, \frac{\partial \theta}{\partial y} = -\gamma_1(1 - \theta); \text{ at } y = 0, x \geq 0, \\ u = u_e(x), \frac{\partial u}{\partial y} = 0, \theta = 0; \text{ as } y \rightarrow \infty, x \geq 0, \end{aligned} \right\} \tag{14}$$

and

$$\left. \begin{aligned} u = 0, v = 0, \frac{\partial \theta}{\partial y} = -1, \text{ at } y = 0, x \geq 0, \\ u = u_e(x), \frac{\partial u}{\partial y} = 0, \theta = 0, \text{ as } y \rightarrow \infty, x \geq 0, \end{aligned} \right\} \tag{15}$$

where Prandtl number, $\text{Pr} = \mu_f C_p / k_f$ and viscoelastic parameter, $K = k_0 U_\infty / \mu_f a$.

3. Mathematical solution

The governing equations (11) to (13) with corresponded BCs (14) and (15) are solved by considering the following variables

$$\psi = xF(x, y), \theta = \theta(x, y), \tag{16}$$

with the stream function ψ

$$u = \frac{\partial \psi}{\partial y}, v = -\frac{\partial \psi}{\partial x} \tag{17}$$

Substitute equations (16) and (17) into equations (11) to (13) yields

$$\begin{aligned} &\left[(1-\varphi) + \varphi \frac{\rho_s}{\rho_f} \right] \left[\left(\frac{\partial F}{\partial y} \right)^2 + x \frac{\partial F}{\partial y} \left(\frac{\partial^2 F}{\partial x \partial y} \right) - x \frac{\partial F}{\partial x} \frac{\partial^2 F}{\partial y^2} - F \frac{\partial^2 F}{\partial y^2} \right] \\ &= \left[(1-\varphi) + \varphi \frac{\rho_s}{\rho_f} \right] \frac{\sin x \cos x}{x} + \frac{1}{(1+\varphi)^{2.5}} \frac{\partial^3 F}{\partial y^3} + \left[(1-\varphi) + \varphi \frac{(\rho\beta)_s}{(\rho\beta)_f} \right] \lambda \theta \frac{\sin x}{x} \\ &+ K \left[2 \frac{\partial F}{\partial y} \frac{\partial^3 F}{\partial y^3} - F \frac{\partial^4 F}{\partial y^4} - \left(\frac{\partial^2 F}{\partial y^2} \right)^2 + x \left(\frac{\partial^2 F}{\partial x \partial y} \frac{\partial^3 F}{\partial y^3} - \frac{\partial F}{\partial x} \frac{\partial^4 F}{\partial y^4} \right) \right. \\ &\quad \left. + \left(\frac{\partial F}{\partial y} \frac{\partial^4 F}{\partial x \partial y^3} - \frac{\partial^2 F}{\partial y^2} \frac{\partial^3 F}{\partial x \partial y^2} \right) \right], \end{aligned} \tag{18}$$

$$\frac{(k_s + 2k_f) - 2\varphi(k_f - k_s)}{(k_s + 2k_f) + \varphi(k_f - k_s)} \left(1 + \frac{4N_R}{3} \right) \frac{1}{Pr} \frac{\partial^2 \theta}{\partial y^2} + \left[(1 - \varphi) + \varphi \frac{(\rho C_p)_s}{(\rho C_p)_f} \right] F \frac{\partial \theta}{\partial y} = x \left[(1 - \varphi) + \varphi \frac{(\rho C_p)_s}{(\rho C_p)_f} \right] \left(\frac{\partial F}{\partial y} \frac{\partial \theta}{\partial x} - \frac{\partial F}{\partial x} \frac{\partial \theta}{\partial y} \right), \tag{19}$$

with corresponding boundary conditions CBC and CHF, which are,

$$\left. \begin{aligned} F = 0, \quad \frac{\partial F}{\partial y} = 0, \quad \frac{\partial \theta}{\partial y} = -\gamma_1(1 - \theta); \quad \text{at } y = 0, x \geq 0, \\ \frac{\partial F}{\partial y} = \frac{\sin x}{x}, \quad \frac{\partial^2 F}{\partial y^2} = 0, \quad \theta = 0; \quad \text{as } y \rightarrow \infty, x \geq 0, \end{aligned} \right\} \tag{20}$$

and

$$\left. \begin{aligned} F = 0, \quad \frac{\partial F}{\partial y} = 0, \quad \frac{\partial \theta}{\partial y} = -1; \quad \text{at } y = 0, x \geq 0, \\ \frac{\partial F}{\partial y} = \frac{\sin x}{x}, \quad \frac{\partial^2 F}{\partial y^2} = 0, \quad \theta = 0; \quad \text{as } y \rightarrow \infty, x \geq 0, \end{aligned} \right\} \tag{21}$$

Then, equations (18) and (19) are reduced into subsequent form at lower stagnation point of the cylinder ($x \approx 0^\circ$) as follows

$$\frac{1}{(1 + \varphi)^{2.5}} f''' - \left[(1 - \varphi) + \varphi \frac{\rho_s}{\rho_f} \right] [f'^2 - ff''] + K(2f'f''' - ff''v - f'^2) + \left[(1 - \varphi) + \varphi \frac{(\rho\beta)_s}{(\rho\beta)_f} \right] \lambda \theta = 0, \tag{22}$$

$$\frac{(k_s + 2k_f) - 2\varphi(k_f - k_s)}{(k_s + 2k_f) + \varphi(k_f - k_s)} \left(1 + \frac{4N_R}{3} \right) \frac{1}{Pr} \theta'' + \left[(1 - \varphi) + \varphi \frac{(\rho C_p)_s}{(\rho C_p)_f} \right] f \theta' = 0 \tag{23}$$

with dimensionless BCs

$$\left. \begin{aligned} f(0) = 0, \quad f'(0) = 0, \quad \theta'(0) = -\gamma_1(1 - \theta(0)), \\ f'(\infty) = 1, \quad f''(\infty) = 0, \quad \theta(\infty) = 0. \end{aligned} \right\} \tag{24}$$

and

$$\left. \begin{aligned} f(0) = 0, \quad f'(0) = 0, \quad \theta'(0) = -1, \\ f'(\infty) = 1, \quad f''(\infty) = 0, \quad \theta(\infty) = 0, \end{aligned} \right\} \tag{25}$$

The physical quantities of fluid flow are skin friction C_f and heat transfer $\theta_w(x)$. The terms of C_f and $\theta_w(x)$ are denoted by

$$C_f = Re^{1/2} \frac{\tau_w}{\rho U_\infty^2}, \quad \theta_w(x) = Re^{-1/2} \frac{aq_w}{k(T_w - T_\infty)}. \tag{26}$$

with the skin friction τ_w and heat transfer q_w at wall are [55].

$$\tau_w = \mu_{nf} \left(\frac{\partial u}{\partial y} \right)_{y=0} + k_o \left(u \frac{\partial^2 u}{\partial x \partial y} + v \frac{\partial^2 u}{\partial^2 y} + 2 \left(\frac{\partial u}{\partial x} \frac{\partial u}{\partial y} \right) \right)_{y=0}, \quad q_w = -k_{nf} \left(\frac{\partial T}{\partial y} \right)_{y=0} \tag{27}$$

Using dimensionless variables (10), the non-dimensional form of C_f and $\theta_w(x)$ for CBC and CHF are

$$\begin{aligned} C_f(x) &= \frac{1}{(1 - \varphi)^{2.5}} x \left(\frac{\partial^2 F}{\partial y^2} \right)_{y=0}, \quad \theta_w(x) = -\frac{k_{nf}}{k_f} \left(\frac{\partial \theta}{\partial y} \right)_{y=0}, \\ C_f(x) &= \frac{1}{(1 - \varphi)^{2.5}} x \left(\frac{\partial^2 F}{\partial y^2} \right)_{y=0}, \quad \theta(x) = \frac{k_{nf}}{k_f} \theta_w(x). \end{aligned} \tag{28}$$

4. Results and discussion

The governing equations (18) - (19) and (22) - (23) in corresponded BCs (20)–(21) and (24)–(25) are executed via Keller-box techniques numerically. This method has been implemented by many researchers, such as Aurangzaib et al. [56] and Rosali et al. [57] because it is an unconditionally stable and succeed in obtaining the accurate results. It is also recommended to be used in solving the nonlinear parabolic problems. The details of this method are stated in the Cebeci and Bradshaw [58] book. The four steps involved to obtain the numerical results are as follows:

- (i) The ordinary differential equations are reduced to a system of first order equations.

Table 2
Comparison of C_f for λ values with $\gamma_1 = 1000$, $Pr = 1$, $K = 0$, $\varphi = 0$ and $N_R = 0$ in CBC case.

λ	Nazar et al. [35]	Kasim et al. [37]	Present results
-0.2	1.0340	1.033028	1.033034
0.4	1.5747	1.573759	1.573749
3.0	2.4913	2.489892	2.489872
10	5.7730	5.777805	5.777701

Table 3
Comparison of $-\theta'$ for λ values with $\varphi = 0$, $Pr = 1$, $K = 0$ and $N_R = 0$ in CHF case.

λ	Merkin [13]	Rashad et al. [59]	Present results
-0.5	0.5420	0.5421	0.541784
0.0	0.5705	0.5706	0.570141
0.5	0.5943	0.5947	0.594164
1.0	0.6158	0.6160	0.615180
2.0	0.6497	0.6518	0.651019
5.0	0.7315	0.7319	0.730881

- (ii) The first order system is discretized to obtain the equations in the finite difference form by using central difference scheme.
- (iii) The nonlinear equations are linearized using Newton's method and then written in matrix-vector form.
- (iv) Finally, the linear system can be solved via block tri-diagonal elimination technique.

The impact of N_R , γ_1 , λ , K and φ on behavior of velocity, skin friction, temperature and thermal transfer rate are studied. The present and previous results by Nazar et al. [35] and Kasim et al. [37] for skin friction and Merkin [13] and Rashad et al. [59] for heat transfer rate are compared for validation process. Tables 2 and 3 displays that all the outputs are discovered in excellent agreement.

The influences of radiation N_R , volume fraction of nanoparticles φ and Biot numbers γ_1 on velocity are observed in Fig. 2(a), (b) and 2(c). The velocity rise with increment of N_R in CHF and CBC cases as displayed in Fig. 2(a). The reason is the thermal energy transferred within the momentum boundary layer thickness enhance as N_R elevates. Hence, the collision between fluid particles become stronger, which cause the fluid velocity accelerates in the flow. The similar graphical results are obtained in the studies by Zokri et al. [60]. Fig. 2 (b) portrays the deceleration on velocity for increasing φ values. Physically, the fluid flow slowing down due to the viscosity of fluid boost as the concentration nanoparticles rises. Furthermore, it is discovered in Fig. 2(c) that the fluid velocity accelerates as γ_1 rises.

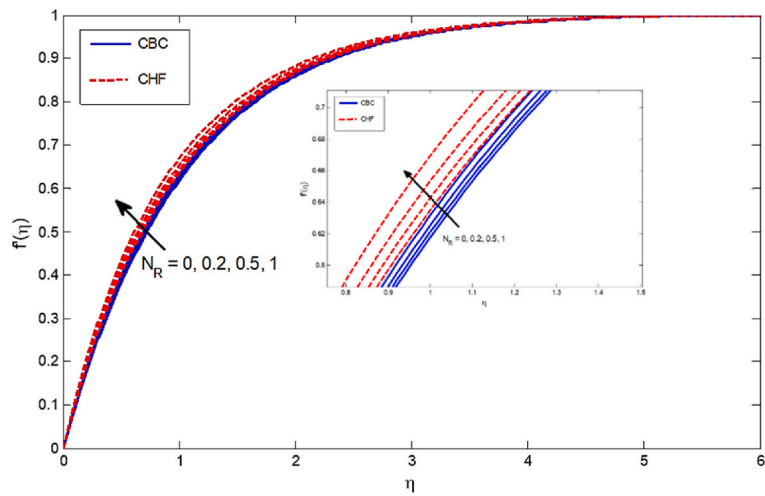
The variation of radiation N_R , volume fraction of nanoparticles φ and Biot numbers γ_1 on temperature are demonstrated in Fig. 3(a), (b) and 3(c) of CHF and CBC conditions. Fig. 3(a) depicts the temperature rises with increment of N_R in CHF and CBC cases. The reason is the thermal energy transferred within the thermal boundary region enhance as N_R elevates. Consequently, the movement of fluid particles accelerates in the flow, which resulting in the temperature of fluid increases. Hence, it is concluded that the minimum radiation value must be applied for rapid cooling process. The fluid temperature enhances with increase of φ as plotted in Fig. 3(b). It is discovered that the collision of nanoparticles accelerates when φ increases, which improves the fluid thermal conductivity and thus boost the temperature in fluid flow. Fig. 3(c) presents the enhancement of temperature with raise of γ_1 , which causes the convection of heat transfer at cylinder surface enhances. The same behavior of profiles is obtained from published works by Hayat et al. [61] and Grosan et al. [62].

Fig. 4(a), (b) and 4(c) demonstrates the impacts of N_R , φ , and γ_1 on the skin friction at various points of x on the cylinder surface. The wall shear stress enhances by increasing N_R values as illustrated in Fig. 4(a). The reason is the velocity of flow accelerates, which resulting in the friction amongst the fluid particles and the cylinder surface elevates. Hence, the skin friction in Fig. 4(a) boosts as N_R and x increases. Fig. 4(b) portrays the raise in volume fraction of nanoparticle improves the fluid viscosity, and thus, elevates the shear stress at boundary surface. Fig. 4(c) presents the skin friction increase in the influences of γ_1 . The higher resistivity of internal heat at the surface lead to the increment of collision of particles in the fluid flow and thus, elevates the shear stress at surface. A similar behavior of graphical results is observed in Rashad et al. [59] works.

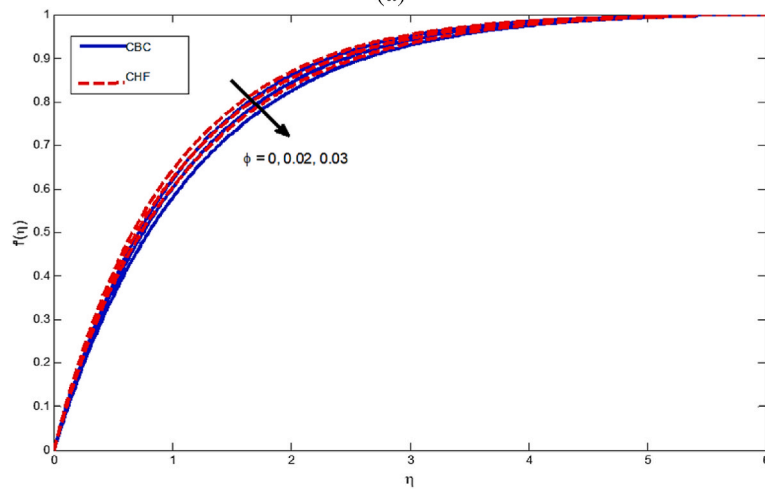
The effects of N_R , φ and γ_1 on the heat transfer rate at various points of x on the cylinder surface are displayed in Fig. 5(a), (b) and 5 (c). The rate of heat transfer rises in the CBC and CHF cases as exhibited in Fig. 5(a)(i) and 5(a)(ii) because thermal radiation elevates the temperature within flow, and therefore enhancing the convective heat transfer in the fluid. Fig. 5(b)(i) and 5(b)(ii) portrays the raise in volume fraction of nanoparticle increase the convective heat transfer for CBC and CHF cases. It is discovered the Nusselt number of CHF values higher compared to CBC because the fluid temperature decrease lead to the convection process for CBC case decelerates. Furthermore, the rate of heat transfer elevates from 5% to 11% for CBC case and 6%–14% for CHF case when the nanoparticles volume fraction varies up to 3%. Fig. 5(c)(i) shows the heat transfer rate elevate when γ_1 rises for CBC cases. The higher convective heat transfer at cylinder plate lead to the increment of temperature in the fluid flow. The time for the rate of heat transfer when $\gamma_1 = 0$ is limited because of the uniform temperature as depicted in Fig. 3(a).

5. Conclusion

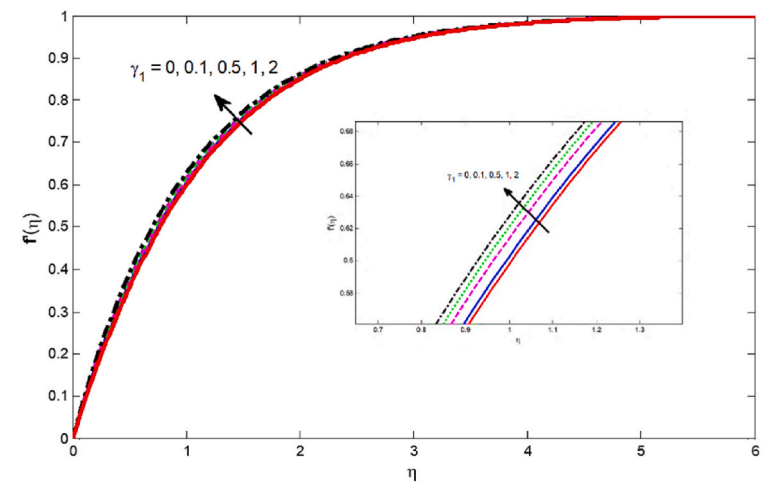
The numerical study of mixed convection flow of Walter's B nanofluid under influences of thermal radiation with CBC and CHF



(a)



(b)



(c)

Fig. 2. Impact of (a) N_R with $\phi = 0.03$, $\gamma_1 = 1$ (b) ϕ with $N_R = 0.2$, $\gamma_1 = 1$ and (c) γ_1 with $\phi = 0.03$, $N_R = 0.2$ on velocity for CHF and CBC with $Pr = 6.2$, $K = \lambda = 1$

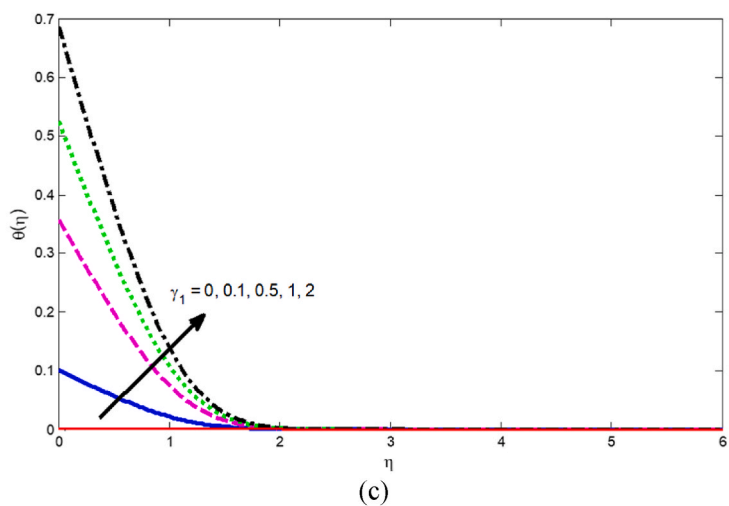
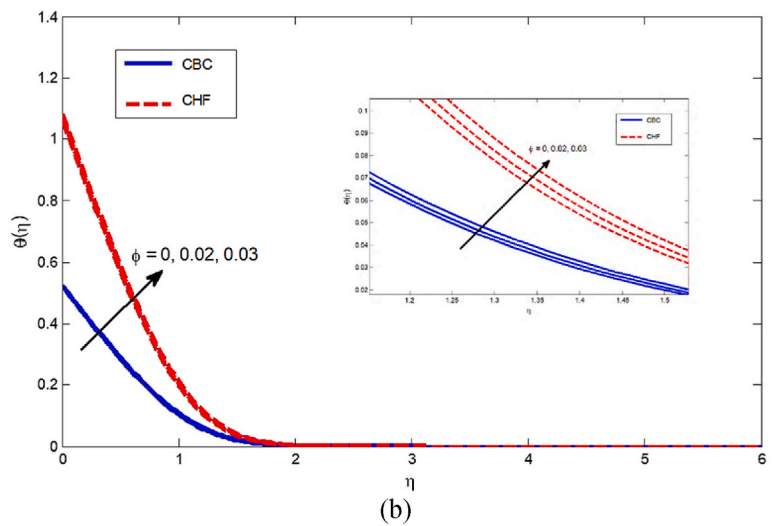
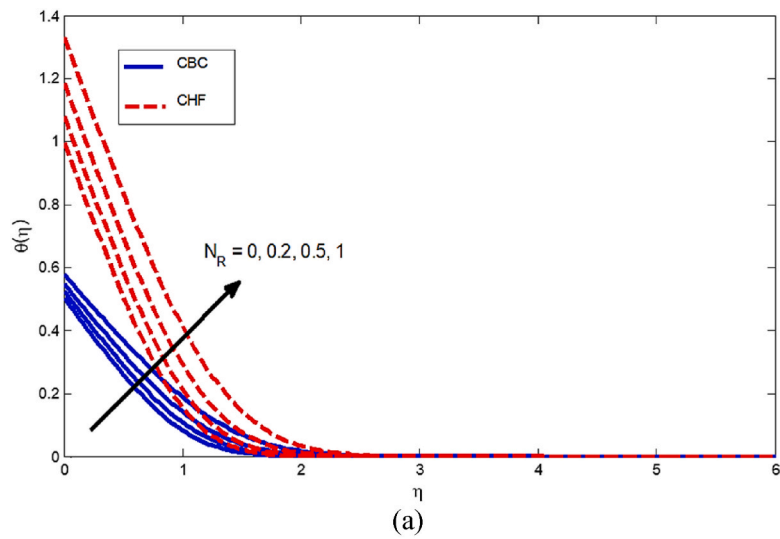


Fig. 3. Impact of (a) N_R with $\phi = 0.03$, $\gamma_1 = 1$ (b) ϕ with $N_R = 0.2$, $\gamma_1 = 1$ and (c) γ_1 with $N_R = 0.2$, $\phi = 0.03$ on temperature for CHF and CBC with $Pr = 6.2$, $K = \lambda = 1$

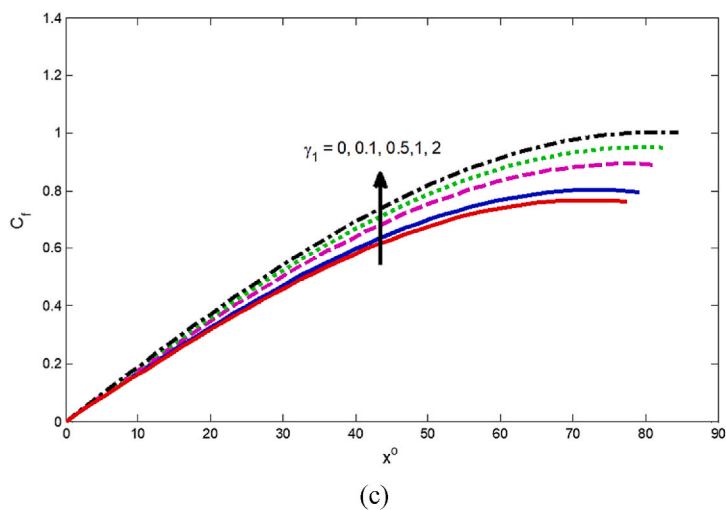
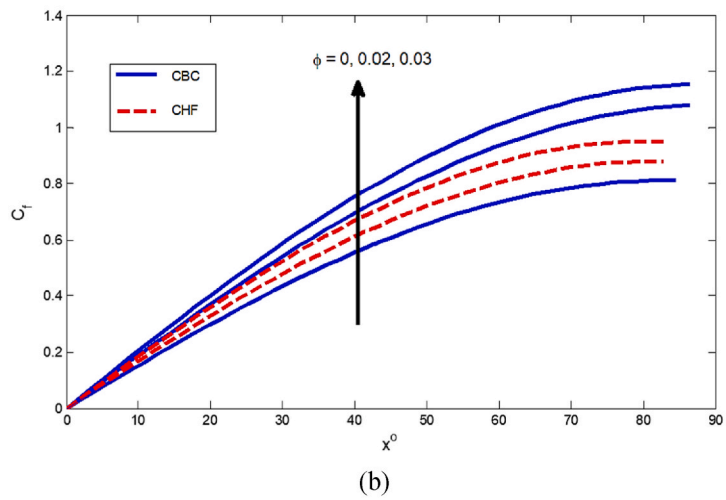
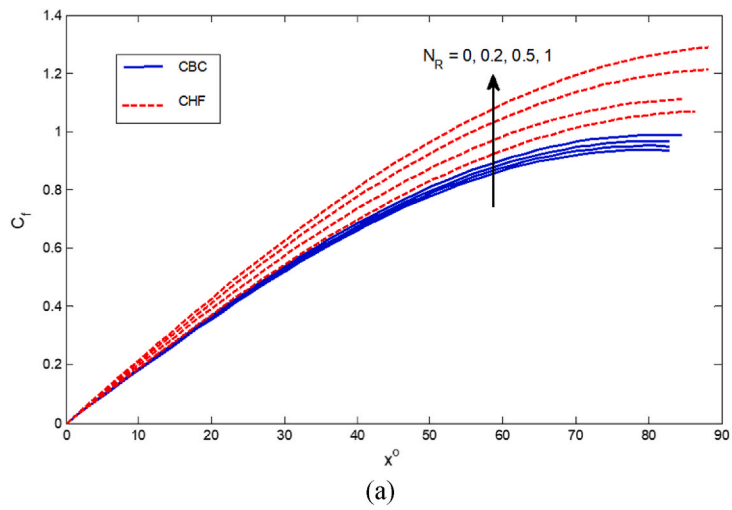


Fig. 4. Impact of (a) N_R with $\phi = 0.03$, $\gamma_1 = 1$ (b) ϕ with $N_R = 0.2$, $\gamma_1 = 1$ and (c) γ_1 with $N_R = 0.2$, $\phi = 0.03$ on skin friction for CHF and CBC with $Pr = 6.2$, $K = \lambda = 1$

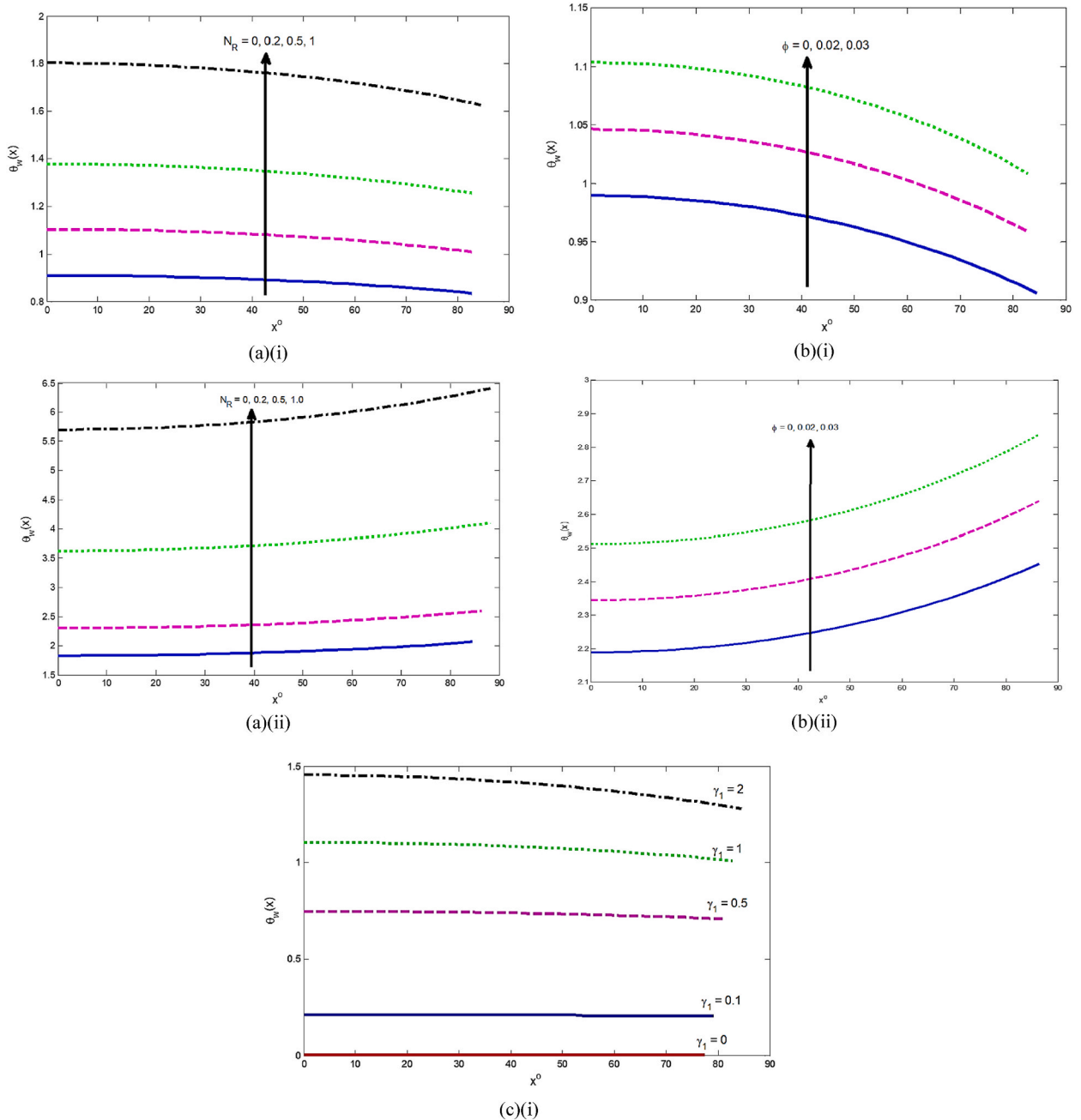


Fig. 5. Impact of (a) N_R with $\phi = 0.03$, $\gamma_1 = 1$ (b) ϕ with $N_R = 0.2$, $\gamma_1 = 1$ and (c) γ_1 with $N_R = 0.2$, $\phi = 0.03$ on rate of heat transfer for (i) CBC and (ii) CHF with $Pr = 6.2$ and $K = \lambda = 1$

conditions is investigated. Transformation of PDEs into ODEs are conducted using suitable non-dimensional variables. Then, the transformed equations are resolved with technique of Keller-box numerically. The behavior flow of velocity, skin friction, temperature and heat transfer rate are plotted and analyzed through MATLAB software graphically. The main conclusions in the analysis are summarized as:

1. The velocity, skin friction, temperature and heat transfer rate increase with raise in N_R for CBC and CHF cases.
2. The increment of ϕ decelerates the fluid velocity and boost the fluid temperature for CBC and CHF cases.
3. The temperature and velocity of fluid enhance for increasing γ_1 values.
4. For CBC and CHF, the heat transfer rate and skin friction for various x position elevates when N_R , ϕ , and γ_1 rises.

5. The CHF magnitude is higher than CBC magnitude due to the convective heat transfer lower in CBC as the fluid temperature slowly dissipate to the surrounding.

Author statement

Category 1:

Conception and design of study: R. Mahat, M. Saqib, N.A.M. Noor, S. Shafie

Acquisition of data: R. Mahat, M. Saqib, N.A.M. Noor, S. Shafie

Analysis and/or interpretation of data: R. Mahat, N.A.M. Noor, I. Khan, S. Shafie.

Category 2.

Drafting the manuscript: R. Mahat, N.A.M. Noor, S. Shafie, M. Saqib

Revising the manuscript critically for important intellectual content: R. Mahat, N.A.M. Noor, I. Khan, S. Shafie.

Category 3.

Approval of the version of the manuscript to be published (the names of all authors must be listed): R. Mahat, N.A.M. Noor, M. Saqib, S. Shafie, I. Khan.

Declaration of competing interest

The authors declare that they have no known competing financial interests or personal relationships that could have appeared to influence the work reported in this paper.

Data availability

No data was used for the research described in the article.

Acknowledgement

The authors would like to acknowledge the Ministry of Higher Education (MOHE) for the financial support through vote numbers, FRGS/1/2019/STG06/UNIKL/03/1.

References

- [1] N.A.M. Noor, S. Shafie, M.A. Admon, MHD squeezing flow of Casson nanofluid with chemical reaction, thermal radiation and heat generation/absorption, *J. Adv. Res. Fluid Mech. Therm. Sci.* 68 (2020) 94–111, <https://doi.org/10.1002/hjt.21587>.
- [2] N.A.M. Noor, S. Shafie, M.A. Admon, Heat and mass transfer on MHD squeezing flow of Jeffrey nanofluid in horizontal channel through permeable medium, *PLoS One* 16 (5) (2021), e0250402, <https://doi.org/10.1371/journal.pone.0250402>.
- [3] N.A.M. Noor, S. Shafie, M.A. Admon, Effects of viscous dissipation and chemical reaction on MHD squeezing flow of Casson nanofluid between parallel plates in a porous medium with Slip Boundary Condition, *Eur. Phys. J. Plus* 135 (2020) 1–24, <https://doi.org/10.1140/epjp/s13360-020-36400868-w>.
- [4] S.U.S. Choi, J.A. Eastman, Enhancing thermal conductivity of fluids with nanoparticles, in: *ASME International, 1995 International Mechanical Engineering Congress & Exposition*, 1995, pp. 99–105. San Francisco, California, USA.
- [5] L. Tham, R. Nazar, I. Pop, Mixed convection boundary layer flow from a horizontal circular cylinder in a nanofluid, *Int. J. Numer. Methods Heat Fluid Flow* 22 (5) (2012) 576–606.
- [6] G.C. Shit, R. Haldar, S.K. Ghosh, Convective heat transfer and MHD viscoelastic nanofluid flow induced by a stretching sheet, *Int. J. Algorithm. Comput. Math.* 2 (2016) 593–608.
- [7] S. Dinarvand, R. Hosseini, I. Pop, Axisymmetric mixed convective stagnation-point flow of a nanofluid over a vertical permeable cylinder by Tiwari-Das nanofluid model, *Powder Technol.* 311 (2017) 147–156.
- [8] M.T. Ghannam, M.N. Esmail, Rheological properties of carboxymethyl cellulose, *J. Appl. Polym. Sci.* 64 (1997) 289–301.
- [9] P.K. Mandal, A.K. Singha, B. Kumar, G.S. Seth, S. Sarkar, Analysis of unsteady Magnetohydrodynamic 3-D rotating flow and transfer of heat in carbon nanotube-water nanofluid: an engineering application, *Journal of Nanofluids* 11 (2) (2022) 204–213.
- [10] S. Nandia, B. Kumbhakar, S. Sarkar, MHD stagnation point flow of $Fe_3O_4/Cu/Ag-CH_3OH$ nanofluid along a convectively heated stretching sheet with partial slip and activation energy: numerical and statistical approach, *Int. Commun. Heat Mass Tran.* 130 (2022), 105791.
- [11] N.A.M. Noor, S. Shafie, M.A. Admon, Unsteady MHD flow of Casson nanofluid with chemical reaction, thermal radiation and heat generation/absorption, *MATEMATIKA* 35 (2019) 33–52, <https://doi.org/10.11113/matematika.v35.n4.1262>.
- [12] D.D. Ganji, S.H.H. Kachapi, Application of Nonlinear Systems in Nanomechanics and Nanofluids: Analytical Methods and Applications Micro and Nano Technologies, William Andrew, United Kingdom, 2015.
- [13] J.H. Merkin, Natural-convection boundary-layer flow on a vertical surface with Newtonian heating, *Int. J. Heat Fluid Flow* 15 (5) (1994).
- [14] S. Salehi, A. Nori, K. Hosseinzadeh and D. D. Ganji, "Hydrothermal analysis of MHD squeezing mixture fluid suspended by hybrid nanoparticles between two parallel plates," *Case Stud. Therm. Eng.*, 100650, 2020.
- [15] G.K. Ramesh, A.J. Chamkha, B.J. Gireesha, Boundary Layer Flow Past an Inclined Stationary/moving Flat Plate with Convective Boundary Condition", *Afrika Matematika*, 2015.
- [16] M.B. Ashraf, T. Hayat, A. Alsaedi, Mixed convection flow of Casson fluid over a stretching sheet with convective boundary conditions and Hall effect, *Bound. Value Probl.* 2017 (1) (2017).
- [17] H. Ahmad, T. Javed, A. Ghaffari, Radiation effect on mixed convection boundary layer flow of a viscoelastic fluid over a horizontal circular cylinder with constant heat flux, *J. Appl. Fluid Mech.* 9 (3) (2016) 1167–1174.
- [18] S.M. Zokri, N.S. Arifin, M.K.A. Mohamed, M.Z. Salleh, A.R.M. Kasim, N.F. Mohammad, Numerical solution on mixed convection boundary layer flow past a horizontal circular cylinder in a Jeffrey fluid with constant heat flux, *AIP Conf. Proc.* 1870 (2017) 1–8.
- [19] N.A.M. Noor, S. Shafie, M.A. Admon, Impacts of chemical reaction on squeeze flow of MHD Jeffrey fluid in horizontal porous channel with slip condition, *Phys. Scripta* 96 (2021) 1–18, <https://doi.org/10.1088/1402-4896/abd821>.
- [20] S. Hosseinzadeh, Kh Hosseinzadeh, A. Hasibi, D.D. Ganji, Hydrothermal analysis on non-Newtonian nanofluid flow of blood through porous vessels, *J. Process Mech. Eng.* 236 (2022) 1604–1615. No. 4.
- [21] R.S. Rivlin, Large elastic deformations of isotropic materials IV. further developments of the general theory, *Phil. Trans. Roy. Soc. Lond. Math. Phys. Sci.* 241 (835) (1948) 379–397.

- [22] B.K. Min, H. Kolsky, A.C. Pipskin, Viscoelastic response to small deformations superposed on a large stretch, *Int. J. Solid Struct.* 13 (8) (1977) 771–781.
- [23] A. Co, R.B. Bird, Slow viscoelastic radial flow between parallel disks, *Appl. Sci. Res.* 33 (5) (1977) 384–404.
- [24] S.R. Mishra, P.K. Pattnaik, M.M. Bhatti, T. Abbas, Analysis of heat and mass transfer with MHD and chemical reaction effects on viscoelastic fluid over a stretching sheet, *Indian J. Phys.* 91 (10) (2017) 1219–1227.
- [25] T. Hayat, S. Asad, M. Mustafa, H.H. Alsulami, Heat transfer analysis in the flow of Walters' B fluid with a convective boundary condition, *Chin. Phys. B* 23 (8) (2014) 1–7.
- [26] S.A.M. Tonekaboni, R. Abkar, R. Khowar, On the study of viscoelastic Walters' B fluid in boundary layer flows, *Math. Probl. Eng.* 2012 (2012) 1–18.
- [27] S.G. Mohiddin, V.R. Prasad, S.V.K. Varma, O.A. Beg, Numerical study of unsteady free convective heat and mass transfer in a Walters-B viscoelastic flow along a vertical cone, *Int. J. Appl. Math. Mech.* 6 (15) (2010) 88–114.
- [28] S. Nadeem, R. Mehmood, S.S. Motsa, Numerical investigation on MHD oblique flow of Walter's B type nano fluid over a convective surface, *Int. J. Therm. Sci.* 92 (2015) 162–172.
- [29] V.R. Prasad, B. Vasu, O.A. Beg, R. Parshad, Unsteady free convection heat and mass transfer in a Walters-B viscoelastic flow past a semi-infinite vertical plate: a numerical study, *Therm. Sci.* 15 (2) (2011) 291–305.
- [30] Q. Al-Mdallal, K.A. Abro, I. Khan, Analytical solutions of fractional Walter's B fluid with applications, *Complexity* 2018 (2018) 1–10.
- [31] O.D. Makinde, M.G. Reddy, K.V. Reddy, Effects of thermal radiation on MHD peristaltic motion of Walters-B fluid with heat source and slip conditions, *J. Appl. Fluid Mech.* 10 (4) (2017) 1105–1112.
- [32] A. Shafiq, Z. Hammouch, A. Turab, Impact of radiation in a stagnation point flow of Walters' B fluid towards a Riga plate, *Therm. Sci. Eng. Prog.* 6 (2018) 27–33.
- [33] M. Javed, T. Hayat, M. Mustafa, B. Ahmad, Velocity and thermal slip effects on peristaltic motion of Walters-B fluid, *Int. J. Heat Mass Tran.* 96 (2016) 210–217.
- [34] A. Harnoy, An investigation into the flow of elastico-viscous fluids past a circular cylinder, *Rheol. Acta* 26 (1987) 493–498.
- [35] R. Nazar, N. Amin, I. Pop, Mixed convection boundary-layer flow from a horizontal circular cylinder with a constant surface heat flux, *Heat Mass Tran.* 40 (2004) 219–227.
- [36] I. Anwar, N. Amin, I. Pop, Mixed convection boundary layer flow of a viscoelastic fluid over a horizontal circular cylinder, *Int. J. Non Lin. Mech.* 43 (9) (2008) 814–821.
- [37] A.R.M. Kasim, N.F. Mohammad, S. Shafie, I. Pop, Constant heat flux solution for mixed convection boundary layer viscoelastic fluid, *Heat Mass Tran.* 49 (2) (2013) 163–171.
- [38] A.R.M. Kasim, M.A. Admon, S. Shafie, Free convection boundary layer flow of a viscoelastic fluid in the presence of heat generation, *World Acad. Sci. Eng. Technol.* 51 (2011) 492–499.
- [39] S. Pramanik, Casson fluid flow and heat transfer past an exponentially porous stretching surface in presence of thermal radiation, *Ain Shams Eng. J.* 5 (1) (2013) 205–212.
- [40] M. Farooq, M.I. Khan, M. Waqas, T. Hayat, A. Alsaedi, M.I. Khan, MHD stagnation point flow of viscoelastic nanofluid with non-linear radiation effects, *J. Mol. Liq.* 221 (2016) 1097–1103.
- [41] K.G. Kumar, B.J. Gireesha, S. Manjunatha, N.G. Rudraswamy, Effect of nonlinear thermal radiation on double-diffusive mixed convection boundary layer flow of viscoelastic nanofluid over a stretching sheet, *Int. J. Mech. Mater. Eng.* 12 (1) (2017) 1–18.
- [42] Z. Khan, I. Khan, M. Ullah, I. Tlili, Effect of thermal radiation and chemical reaction on non-Newtonian fluid through a vertically stretching porous plate with uniform suction, *Results Phys.* 9 (2018) 1086–1095.
- [43] S.M. Ibrahim, P.V. Kumar, O.D. Makinde, Chemical reaction and radiation effects on non-Newtonian fluid flow over a stretching sheet with non-uniform thickness and heat source, *Defect Diffusion Forum* 387 (2018), 319–331.
- [44] A. Hussain, S. Akbar, L. Sarwar, S. Nadeem, Z. Iqbal, Effect of time dependent viscosity and radiation efficacy on a non-Newtonian fluid flow, *Heliyon* 5 (2019), 1–32.
- [45] N.A.C. Sidik, M.M.A.W. Yazid, R. Mamat, Recent advancement of nanofluids in engine cooling system, *Renew. Sustain. Energy Rev.* 75 (October 2016) (2017) 137–144.
- [46] S.A. Tonekaboni, R. Abkar, R. Khowar, 'On the Study of Viscoelastic Walters' B Fluid in Boundary Layer Flows' vol. 2012, *Mathematical Problems in Engineering*, 2012, pp. 1–18.
- [47] Y. Lin, L. Zheng, X. Zhang, Radiation effects on Marangoni convection flow and heat transfer in pseudo-plastic non-Newtonian nanofluids with variable thermal conductivity, *Int. J. Heat Mass Tran.* Elsevier Ltd 77 (2014) 708–716.
- [48] C. Bardos, F. Golse, B. Perthame, The Rosseland approximation for the radiative transfer equations, *Commun. Pure Appl. Math.* 40 (6) (1987) 691–721.
- [49] S.H.F.M. Kanafiah, A.R.M. Kasim, S.M. Zokri, M.R. Ilias, Combined convective transport of brinkman-viscoelastic fluid across horizontal circular cylinder with convective boundary condition, *J. Adv. Res. Fluid Mech. Therm. Sci.* 89 (2) (2022) 15–24.
- [50] S.M. Zokri, N.S. Arifin, M.K.A. Mohamed, A.R.M. Kasim, N.F. Mohammad, M.Z. Salleh, Mathematical model of mixed convection boundary layer flow over a horizontal circular cylinder filled in a Jeffrey fluid with viscous dissipation effect, *Sains Malays.* 47 (7) (2018) 1607–1615.
- [51] R.D. Selvakumar, S. Dhinakaran, Nanofluid flow and heat transfer around a circular cylinder: a study on effects of uncertainties in effective properties, *J. Mol. Liq.* 223 (2016) 572–588.
- [52] Y. Jaluria, "HMT the Science and Applications of Heat and Mass Transfer: Report, Review and Computer Programs," Pergamon Press, New York.
- [53] Aurangzaib, A.R.M. Kasim, N. Mohammad, S. Shafie, Unsteady MHD mixed convection stagnation point flow in a micropolar fluid on a vertical surface in a porous medium with Soret and Dufour effects, *Heat Tran. Res.* 44 (7) (2013).
- [54] H. Rosali, A. Ishak, R. Nazar, J. Merkin, I. Pop, The effect of unsteadiness on mixed convection boundary-layer stagnation-point flow over a vertical flat surface embedded in a porous medium, *Int. J. Heat Mass Tran.* 77 (2014) 147–156.
- [55] T. Cebeci, P. Bradshaw, *Physical and Computational Aspects of Convective Heat Transfer*, Springer, New York, 1988.
- [56] A.M. Rashad, A.J. Chamkha, M. Modather, Mixed convection boundary-layer flow past a horizontal circular cylinder embedded in a porous medium filled with a nanofluid under convective boundary condition, *Comput. Fluid* 86 (2013) 380–388.
- [57] S.M. Zokri, N.S. Arifin, M.K.A. Mohamed, M.Z. Salleh, A.R.M. Kasim, W.N.S.W. Yusoff, N.F. Mohammad, Influence of radiation and viscous dissipation on magnetohydrodynamic Jeffrey fluid over a stretching sheet with convective boundary conditions, *Malays. J. Fund. Appl. Sci.* 13 (3) (2017) 279–284.
- [58] T. Hayat, S.A. Shehzad, A. Alsaedi, M.S. Alhothuali, Mixed convection stagnation point flow of Casson fluid with convective boundary conditions, *Chin. Phys. Lett.* 29 (11) (2012) 1147041–1147044.
- [59] T. Grosan, J.H. Merkin, I. Pop, Mixed convection boundary-layer flow on a horizontal flat surface with a convective boundary condition, *Meccanica* 48 (9) (2013) 2149–2158.